Jundishapur J Nat Pharm Prod. In Press(In Press):e101013. doi: 10.5812/jjnpp.101013.

Published online 2021 March 30. **Research Article**

Oregano (*Origanum vulgar* subsp. *viride*) Essential Oil: Extraction, Preparation, Characterization, and Encapsulation by Chitosan-Carbomer Nanoparticles for Biomedical Application

Mona Sharififard [1, 2], Maryam Kouchak [3, 4], Ismaeil Alizadeh [1, 5, *] and Elham Jahanifard [1, 2]

[1] Infectious and Tropical Diseases Research Center, Health Research Institute, Ahvaz Jundishapur University of Medical Sciences, Ahvaz, Iran
[2] Department of Medical Entomology and Vector Control, School of Public Health, Ahvaz Jundishapur University of Medical Sciences, Ahvaz, Iran
[3] Nanotechnology Research Center, Ahvaz Jundishapur University of Medical Sciences, Ahvaz, Iran
[4] Department of Pharmaceutics, School of Pharmacy, Ahvaz Jundishapur University of Medical Sciences, Ahvaz, Iran
[5] Department of Vector Biology and Control, Faculty of Public Health, Kerman University of Medical Sciences, Kerman, Iran

[*] *Corresponding author*: Infectious and Tropical Diseases Research Center, Health Research Institute, Ahvaz Jundishapur University of Medical Sciences, Ahvaz, Iran. Email: ismaeil.alizadeh@yahoo.com

Received 2020 January 28; **Revised** 2020 August 03; **Accepted** 2020 August 11.

Abstract

Background: Plant essential oils (EOs) as natural agents have broad activities, including antibacterial, antifungal, antiviral, insecticidal, and repel activities because of their chemical compositions.
Objectives: The objective of this study was to increase the stability of *Origanum vulgar* subsp. *viride* EOs by encapsulation in chitosan-carbomer nanoparticles by ionic gelation method.
Methods: The EOs from dried leaves of *O. vulgar* subsp. *Viride* were extracted by hydro-distillation method, and EO components were determined by gas chromatography-mass spectrometry (GC-MS). Besides, OEO-loaded chitosan (CS) nano-capsules were prepared using the ionic gelation method. The molecular structure and morphology of nanoparticles were characterized by Fourier Transform-Infrared (FTIR) and scanning electron microscopy (SEM), respectively. The encapsulation efficiency (EE), loading capacity (LC) of the OEO-loaded CS nanoparticles, and their release profiles were determined using UV/Vis spectrophotometry.
Results: The major components of OEO were thymol (20.53%), 4-terpinenol (20.28%), and γ-terpinene (12.22%). The percentages of EE and LC of OEO ranged from 99.25 $\pm$ 0.74 to 93.84 $\pm$ 0.71 and 38.02 $\pm$ 0.18 to 66.73 $\pm$ 0.51, respectively, with increasing the OEO to chitosan ratio from 1:0.01 to 1:0.04 W/V. The nanoparticles were regular, uniform, and spherical in shape with an average size of 134 to 181 nm, which were dispersed throughout the solution. The zeta potential values for blank chitosan nanoparticles (CSNPs) and OEO-loaded CSNPs were +23.4 and +38.5 mV, respectively.
Conclusions: The results confirmed the suitability of the CS-carbomer complex for OEO- CSNPs formation. It is recommended to evaluate the antimicrobial, insecticidal and insect repel activities of developed OEO nanoparticles in laboratory and field studies.

Keywords: *Origanum vulgar*, Encapsulation, Nanoparticles, Chitosan, Carbomer

1. Background

Plants essential oils (EOs) as natural agents are increasingly considered as potential and safe alternatives to chemical products in the medical, pharmaceutical, and agricultural fields. Essential oils have broad biological and antimicrobial activities, including antibacterial, antifungal, antiviral, insecticidal, and repellency activities due to chemical constituents, which are often made up of more than 100 different terpenic compounds (1-5). Most plant-based bioactive compounds are highly sensitive to environmental factors, including oxygen, light, and high temperature. They are volatile, evaporative, and unstable during preparation, utilization, and storage (2, 5-9).

The release rate of plant EOs is usually affected by environmental conditions such that too little release or excessive release causes inefficiency or uncomfortable feelings, respectively (9). Therefore, the development of new formulations that lead to the constant release of EOs under different environmental conditions has been represented over the last few years as an important challenge (9). The susceptibility and low stability of these bioactive compounds can be improved during processing, storage, and consumption using nanotechnology in the form of nanoparticles (NPs). This technology has been widely used in various industries, including food and nutraceutical industries, recently (3). The utilization of liposomes, nano-

emulsions, lipid nanoparticles, and polymeric nanoparticles in nanostructure systems entails some advantages, such as improved drug efficacy and drug bioavailability, reduced adverse effects such as toxicity and irritation, and increased drug stability (10). Moreover, the formulation of EOs as nano-capsules preserves the active ingredients from the degradation by light and heat, which ultimately leads to an increase in its stability, half-life, and biological activity and provides the ability to sustain the release (8, 9, 11, 12). Nanocarriers can potentially protect plant EOs from oxidation and evaporation. In addition, the antimicrobial activity of EOs is facilitated by the various permeability properties of biological membranes due to the nano-scale of the particles (4, 8, 11). Polysaccharide compounds, including hydrogel and chitosan, are generally used for developing nanoparticles for drug delivery in medical and pharmaceutical fields, as well as in the form of pesticides and fertilizers in agriculture (1, 13). Many studies have been conducted to analyze plant EO components and develop appropriate formulations using nanoparticle technologies for increasing the effectiveness of EOs for in vivo applications (1, 3, 14-18). The encapsulation of *Mentha piperita* EOs in chitosan-cinnamic acid nanogel could affect stability and enhance antifungal activity of EOs against *Aspergillus flavus* (15). Oregano EOs were encapsulated in chitosan nanoparticles by a two-step method, i.e., oil-in-water emulsion and ionic gelation of chitosan with sodium tripolyphosphate (TPP), resulting in good characteristics of obtained nanoparticles (3).

2. Objectives

The goal of this study was to develop a nano-capsule formulation containing *Origanum vulgar* subsp. *viride* using the chitosan-carbomer ion gelation method. Moreover, in the present work, OEO-loaded CSNPs were characterized by FTIR. The shape of NPs was determined by SEM. Also, LC, EE, the zeta potential of NPs, and release profiles of OEO from CS nanoparticles were investigated using UV-Vis spectrophotometry.

3. Methods

3.1. Chemical Compounds

Chitosan with deacetylation degree of 97% and viscosity grade of < 25 cp was purchased from Primex (Iceland). Carbomer (Carbopol 940 NF) was obtained from Fluka (Switzerland). Glacial acetic acid, dichloromethane, and Tween 80 were supplied by Merck Chemicals Co. (Germany).

3.2. Plant Sample and EOs Extraction

Origanum vulgar subsp. *viride* was collected from Ashkezar, Yazd Province (latitudes 53°59 and longitudes 31°50), Iran, in May 2017 (Figure 1). The essential oil was extracted from dried leaves by the hydro-distillation method using a Clevenger-type apparatus (Model BP, British Pharmacopoeia, Manufacturer Pyrex Fan Company, Iran) at 90 $\pm$ 5°C for 5 h and was stored at 4°C in dark conditions for experiments (19).

3.3. Essential Oil Yield

The essential oil yield (Y) of the oregano plant was calculated using the following formula (14):

$$Y = \frac{Mass\ of\ the\ extracted\ EO\ (g)}{Mass\ of\ dried\ herb\ (g)} \times 100 \quad (1)$$

3.4. GC-MS Analysis of OEO

Gas Chromatography-Mass Spectrometry (GC-MS) (Hewlett-Packard 6890, Agilent Technology, Santa Clara, California, USA) with characteristics shown in Table 1 was used to identify OEO components (20).

Table 1. General Information on GC-MS Analysis

Characteristics	Conditions
Column type	HP-5MS, (30 m × 0.25 mm × 0.25 μm)
Injection volume, μL	0.1
Initial temperature, °C	40
Injection temperature, °C	260
Detector temperature, °C	270
Mode of injection	Split
Vector gas, %	
Helium	99.999

3.5. Preparation of OEO-Loaded Chitosan Nanoparticles (CSNPs)

The Ion Gelation method was used to prepare chitosan nanoparticles containing OEO. First, CS solution 1% (W/V) was prepared in acetic acid 1% (W/V) and then kept in a closed container under laboratory conditions (23°C - 25°C) for one day. The solution was then centrifuged at 20,000 rpm (model: Vs-35SMTi) for 30 min at 4°C. The supernatant was separated and filtered with filter paper. Afterward, 200 mg of Tween-80 was dissolved in 5 mL of each solution by a steamer heater at 45°C. Volumes of 80, 160, 240, or 320 μL of OEO were dissolved separately in 1 mL of dichloromethane and then added drop-wise to 5 mL of chitosan solution in the ice bath. The obtained emulsion was then added to 25 mL of 4% (W/V) carbomer as droplets in the ice bath (3). This process was performed three times. Figure 2 schematically demonstrates how to prepare OEO-loaded CSNPs.

Figure 1. A, *Origanum vulgar* subsp. *Viride*; B, Dried leaves in a 1 L flask; and C, Extracted EOs

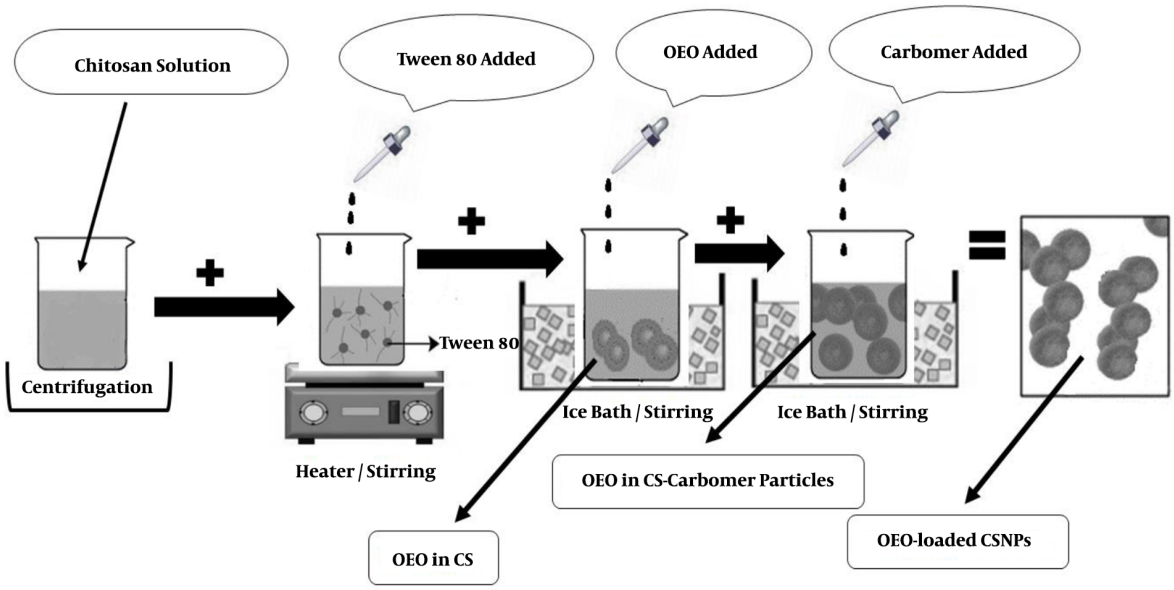

Figure 2. Preparation of OEO-loaded CSNPs by ion gelation method

3.6. Particle Size and Zeta Potential

To determine the particle size and zeta potential of the formulation, a dilute solution of chitosan nanoparticles containing OEO (1:500) was prepared. The nanoparticle size was determined using a laser light scattering (LLS)

apparatus with a wavelength of 633 nm. Also, zeta potential and Polydispersity Index (PDI) measurements were performed by a Zeta seizer (Zeta sizer-nano zs-zen 3600, Malvern instrument). All measurements were performed three times and the average particle size and average zeta potential were calculated.

3.7. Scanning Electron Microscopy (SEM)

Scanning electron microscope (model: 1455VP) was used to investigate the ultrastructure of nanoparticles. A diluted solution (1:500) was brushed to an aluminum foil piece and dried at room temperature. The specimens were then covered with a thin layer of gold and photographed by the scanning electron microscope.

3.8. Fourier Transform Infrared Spectroscopy

The Fourier transform infrared spectroscopy (FTIR) analysis was done on the CS powder, OEO, and OEO-loaded CSNPs using an FTIR device (Vertex 70/80).

3.9. Encapsulation Efficiency and Loading Capacity

The encapsulation efficiency (EE) and loading capacity (LC) of OEO-loaded CSNPs were determined indirectly. The preparations were centrifuged at 20,000 rpm for 30 min at 4°C. The supernatant was then diluted to 1:10 with ethanol 96%, and the content of OEO was determined by a UV/Vis spectrophotometer (Biochrom, WPA, UK) at 275 nm. Calibration curves were prepared using the diluted supernatant of blank nanoparticles containing different concentrations of OEO in ethanol 96% ($R^2 = 0.995$) (3). The EE was calculated using the following equation:

$$EE\,(\%) = \frac{Initial\ amount\ of\ OEO - free\ amount\ of\ OEO}{Initial\ amount\ of\ OEO} \times 100 \quad (2)$$

Also, to determine the LC, the precipitate from centrifugation was separated, dried, and weighed, and the LC was calculated according to the following equation:

$$LC\,(\%) = \frac{Initial\ amount\ of\ OEO - free\ amount\ of\ OEO}{Weight\ of\ nanoparticles\ after\ freeze-drying} \times 100 \quad (3)$$

3.10. In Vitro Release Studies

First, OEO-loaded CSNPs were dispersed separately in ethanol, placed in a microtube, and centrifuged. Then, 5 mL of the supernatant was picked up. The release potential of the OEO-loaded CSNPs was investigated daily using a spectrophotometer at 275 nm for two weeks. The in vitro release studies were performed in triplicate (15).

3.11. Statistical Analysis

In this study, EE%, LC%, and mean particle size of OEO-loaded chitosan nanoparticles were measured in triplicate, and the results were expressed as the mean ± standard deviation (SD). Statistical analysis of data was performed using one-way ANOVA, followed by Tukey's test using SPSS ver. 20. Charts and graphs were plotted by Excel software (Microsoft Office 2013).

4. Results

4.1. EO Yield

The yield of the oregano plant was 1% (V/W) of yellow EO extracted from the dry leaf by hydrostatic method (Figure 1C).

4.2. Chemical Composition of OEO

The composition of OEO was analyzed using GC-MS, and 65 compounds were found (Table 2). The major components were thymol (20.53%), 4-terpinenol (20.28%), γ-terpinene (12.22%), α-terpinene (8.53%), trans-sabinene hydrate (4.42%), α-terpinenol (4.21%), and carvacrol (3.9%).

4.3. Encapsulation Efficiency and Loading Capacity

The percentages of EE and LC of different formulations calculated using Equations 2 and 3 respectively, are shown in Table 3. The EE percentage of OEO ranged from 93.84 ± 0.71 to 99.25 ± 0.74. Overall, by increasing initial OEO content, EE% tended to decrease (P = 0.000). Moreover, the LC percentage of OEO ranged from 38.02 ± 0.18 to 66.73 ± 0.51, and by increasing initial OEO content, LC% tended to increase (P = 0.001). The maximum EE% and LC% values were obtained from the ratios of 1:0.01and 1:0.04 W/V of CS: OEO which were calculated as 99.25±0.74 and 66.73 ± 0.51 %, respectively (Table 3).

4.4. Shape and Size of OEO-loaded Chitosan Nanoparticles

The average size of produced OEO capsules was in the nano-size range which varied from 134 nm to 181 nm depending on OEO volume (Table 3), which increased by increasing OEO content (P = 0.008). The results also showed that with increasing loading of OEO in chitosan nanoparticles, their sizes also increased (P = 0.019).

In addition, scanning electron microscopy was used to investigate the morphology of the nano-capsules produced. The results showed that the nano-capsules were spherical, regular, and uniform in shape and scattered throughout the solution (Figure 3A).

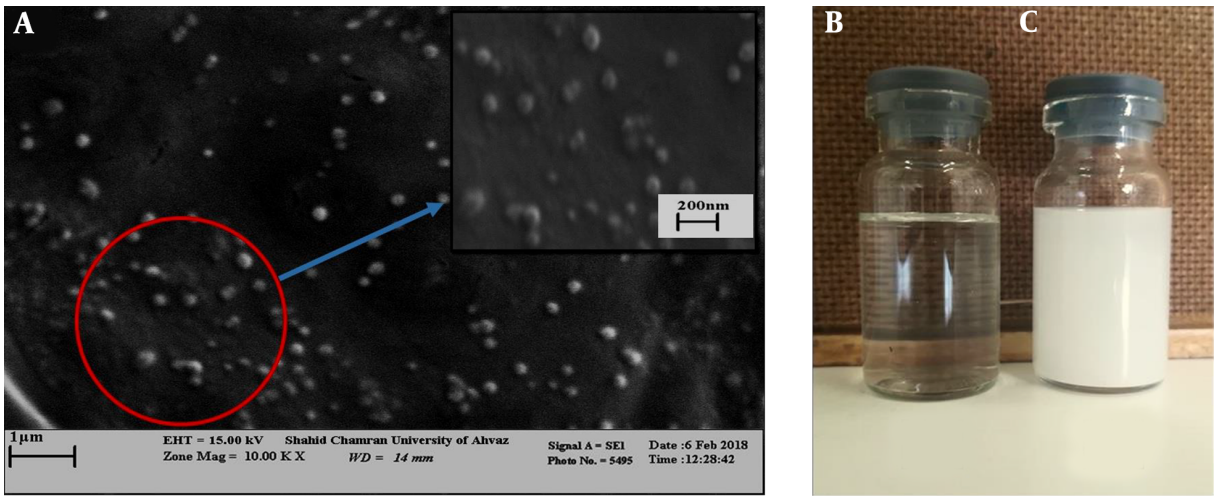

Figure 3. A, SEM image of OEO-loaded chitosan nanoparticles; B, Blank CSNPs; and C, OEO-loaded chitosan nanoparticle solutions

4.5. Particle Size, Polydispersity, and z-Potential Measurements

Some physicochemical characteristics such as Zeta potential (ZP), mean particle size (MPS), and polydispersity index (PDI) of blank CSNPs and OEO-loaded CSNPs (Figure 3B and C) with the weight ratio of 1:0.03 (CS to OEO) are shown in Table 4. The results revealed that the zeta potential values of blank CSNPs and EO-loaded CSNPs were +23.4 and +38.5 mV, respectively. The results showed that the mean particle size and PDI of OEO- loaded CSNPs were 104.1 nm and 0.876, respectively. Zeta potential values were above + 20 mV in blank CSNPs and OEO-loaded CSNPs, which predicted the long-term stability of the provided formulations. In addition, the results showed only one spectrum in blank CSNPs but two spectra in OEO-loaded CSNPs (Figure 4).

4.6. FTIR Characterization

The FTIR analysis results of chitosan powder, chitosan nanoparticles, OEO, and OEO-loaded CSNPs are shown in Figure 5. The CS powder showed characteristic peaks at 3439 cm^{-1} (-OH and -NH2 stretching), 2920 cm^{-1} (-CH stretching), 1653 cm^{-1} (amide I), and 1081 cm^{-1} (C-O-C stretching) (Figure 5A). Pure OEO spectra showed sharp characteristic peaks at 2961 (-CH stretching), 1514 (-N-H bending), 1449 (CH2 bending), 1253 (C-O-C stretching), 1117 (C-O-C stretching), and 937 cm^{-1} (C-H bending) (Figure 5B). For the blank, the amide I (-NH2 bending) peak changed from 1647 to 1641 cm^{-1}, and new peaks appeared at 1259 cm^{-1} (C-N stretch), indicating complex formation through electrostatic interactions between the NH3+ C groups of CS and the phosphoric groups of carbomer in nanoparticles of CSNPs (Figure 5C). These peaks also appeared in the spectra of the provided OEO formulation at nearly the same wave numbers, indicating no interaction between OEO and CSNPs (Figure 5D).

4.7. Release Studies of OEO-Loaded CSNPs

The release profiles of OEO-loaded formulations are shown in Figure 6. All formulations presented a prolonged release during two weeks.

5. Discussion

Environmental and genetic factors may play an important role in determining plant components (16). Our results indicated that major components of EOs of *O. vulgare* subsp. *viride* were thymol, 4-terpinenol, and γ-terpinene. Linalyl acetate (20.1%), sabinene (13.4%), γ-terpinene (5.6%), trans-ocimene (3.6%), and cis-ocimene (3.4%) were reported as the main components of EOs extracted from *Origanum vulgare* subsp. *viride* (20). Also, thymol (29.9%), γ-terpinene (13.0%), β-pinene (11.3%), 3-octanone (9.2%), carvacrol (5.2%), sabinene (5.0%), and α-pinene (4.5%) were introduced as the main compounds of *Origanum vulgare* subsp. *viride* (17). In another study, thymol (28% - 32%), 4-terpineol (10% - 12%), and α-terpinene (7.5% - 10%) were determined as the most frequent compounds (14). Mehdizadeh et al. (16) detected six major compounds, including thymol (21.6 %), 4-terpineol (15.85 %), trans-sabinene hydrate (7.91 %), pcymene (5.69 %), γ-terpinene (5.46 %), and Sabinene (3.81 %) as the main constituents of EOs of *Origanum vulgare* subsp. *viride*. The geographic situation, climate condition, plant origin, harvest season, sampling, and extraction methods may result in different components of *Origanum vulgare* subsp. *viride* (21). Our results also suggested

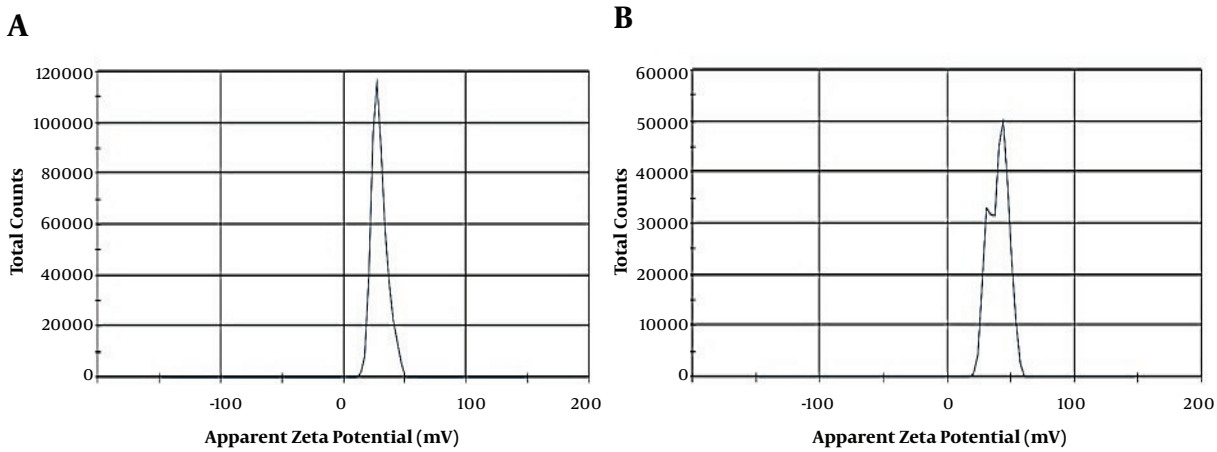

Figure 4. Zeta potential of blank CSNPs (A) and OEO-loaded CSNPs (B) with chitosan to OEO ratio (W/V) of 1:0.03.

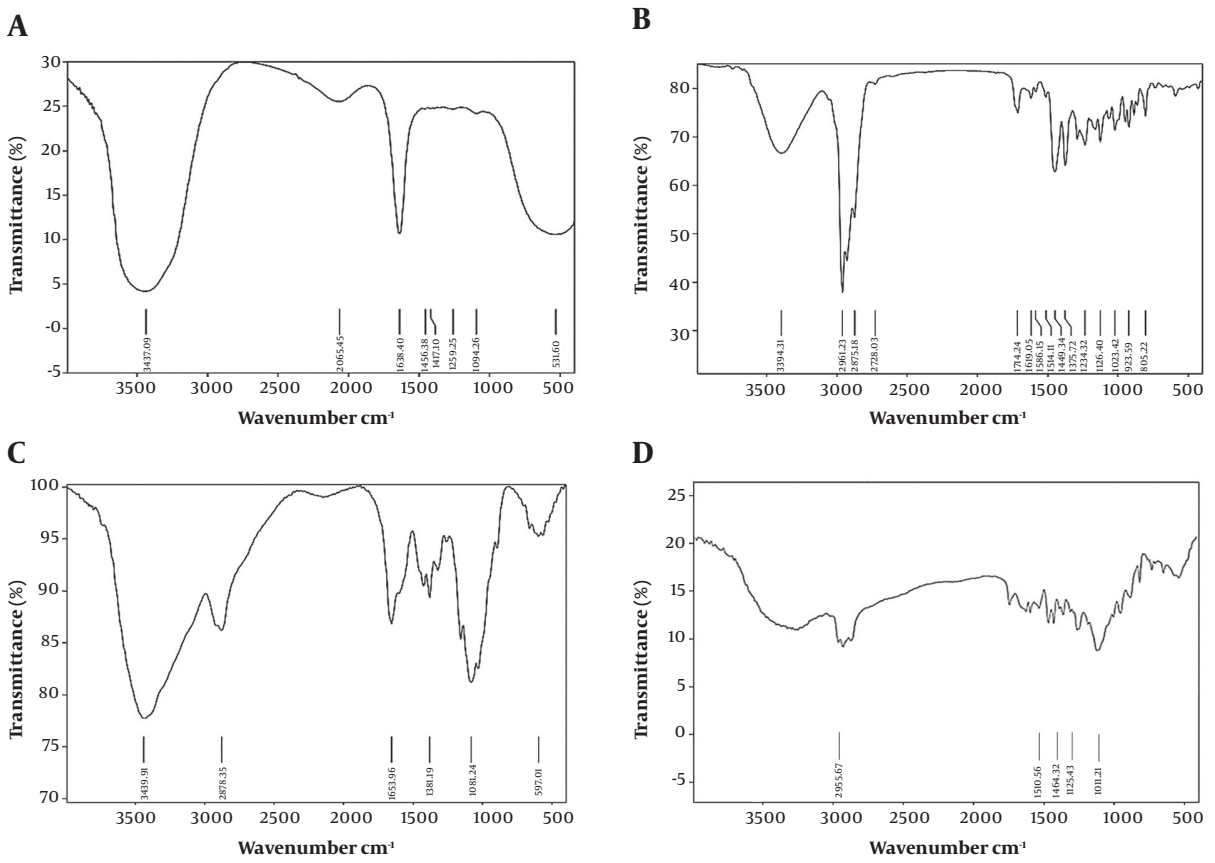

Figure 5. Fourier transform-infrared spectroscopic (FTIR) spectra of (A) chitosan powder, (B) OEO, (C) blank CSNPs, and (D) OEO-loaded chitosan nanoparticles with chitosan to OEO ratio (W/V) of 1:0.03.

that the saturation of the OEO loading solution may result in a decrease in the encapsulation efficiency of chitosan nanoparticles. This finding is in agreement with previous reports (3, 6, 22, 23).

Table 2. Chemical Composition of *Origanum vulgar* subsp. *viride* EOs Analyzed by GC-MS

Numbers	Compound	Retention Time, min	Composition, %
1	α-thujene	7.733	1.75
2	α-pinene	7.916	0.62
3	Sabinene	9.061	5. 6
4	β-pinene	9.145	0.31
5	β-myrcene	9.587	0.57
6	β-phellandrene	9.959	0.3
7	α-terpinene	10.325	8.53
8	p-cymene	10.560	1.96
9	β-phellandrene	10.961	1.91
10	γ-Terpinene	11.590	12.22
11	trans-sabinene hydrate	11.830	4.42
12	α-terpinolene	12.465	1.73
13	cis-sabinene hydrate	12.768	2.09
14	4-terpinenol	15.901	20.28
15	α-terpinenol	15.452	4.21
16	Trans-piperitol	15.589	0.51
17	Bornyl acetate	18.502	0.34
18	Thymol	34.929	20.53
19	Carvacrol	36.495	3.9
20	Caryophyllene	41.801	2.05
21	Spathulenol	51.512	0.74
22	Other compounds	-	9.64

Table 3. Encapsulation Efficiency (EE%) and Loading Capacity (LC%) of OEO in OEO-Loaded Chitosan Nanoparticles Determined by UV-Vis Spectrophotometry and Mean Particle Size of OEO-loaded Chitosan Nanoparticles (N = 3)[a]

Chitosan:OEO Ratio (w/v)	UV-Vis Spectrophotometry	Mean Particle Size, nm	
		EE, %	LC, %
1: 0	0	0	134 ± 20.1
1:0.01	99.25 ± 0.74	38.02 ± 0.18	147 ± 24.6
1:0.02	97.73 ± 0.78	57.91 ± 0.46	163.3 ± 11.5
1:0.03	96.45 ± 6.28	67.20 ± 0.56	164 ± 10.4
1:0.04	93.84 ± 0.71	66.73 ± 0.51	181 ± 11.1

[a]Values are expressed as mean ± SD.

Table 4. Physicochemical Characterization of Blank CSNPs and OEO-Loaded CSNPs With CS to OEO Ratio (W/V) of 1:0.03

Formulation	ZP, mV	MPS, nm	PDI
Blank CSNPs	23.4+	241.2	0.512
OEO-loaded CSNPs	38.5+	104.1	0.876

Abbreviations: MPS, mean particle size; PDI, polydispersity index; ZP, Zeta potential.

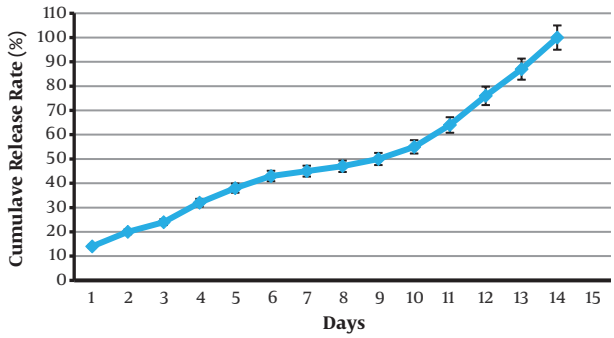

Figure 6. Release profile of OEO-loaded CSNPs during 14 days (two weeks)

The unique features of CS, as a cationic polysaccharide, make it a functional substance to develop chitosan-based products, especially in agriculture, food, industry, biotechnology, and medical science (5, 15, 24). The SEM photographs of the obtained OEO-loaded nanoparticles showed regular, uniform, and spherical nanoparticles in shape and dispersion with particle sizes ranging from 134 to 181 nm. According to Hoesseini et al. (3), OEO nanoparticles exhibited regular distribution and spherical shape with a size range of 40 - 80 nm determined by AFM but the particle size varied from 309.8 to 402.2 nm by laser light scattering technique. The encapsulation of *M. piperiata* EOs in CS-Ci nanogel resulted in nanoparticle sizes of $\leq$ 100 nm. Several studies have documented that increasing loading of EOs in chitosan will result in nanoparticle size increase (3, 14, 25). The swelling of the chitosan layer surrounding particles and/or the aggregation of particles while dispersed in water might result in the larger diameter of chitosan nanoparticles.

The encapsulation efficiency and loading capacity of OEO-loaded chitosan nanoparticles were about 99.2 - 93.8 and 38.02 - 66.73, respectively, when the initial OEO content was 0.01 - 0.04:1 chitosan (v/w). Besides, EE and LC percentages of OEO nanoparticles were obtained as 47% - 21% and 3% - 8%, respectively, in Hoeseeini et al. (3) study when the initial OEO content was 0.1 - 0.8 g/g chitosan. The decrease in EE% with initial OEO content might be the result of the saturation of EOE loading into chitosan nanoparticles. The LC% increased as a function of the initial content of OEO. This finding was in agreement with previous reports (3, 6, 14, 15).

Zeta potential values for blank CSNPs and OEO-loaded CSNPs were +23.4 and +38.5 mV, respectively, which led to

good colloidal stability due to electrostatic repulsive interaction between nanoparticles (24, 26). The zeta potential values for chitosan nanomaterials ranged from +22 to +88 mV (24). Previous studies also confirm our findings (7, 27-29). Moreover, the mean particle size and PDI of OEO-loaded CSNPs were 104.1 nm and 0.876, respectively. In general, the CSNP mean particle size has been reported in the range of 40 - 500 nm previously (1, 3). The PDI value > 0.5 indicated that CSNPs had a broad size distribution (30).

The FTIR analysis indicated that OEO might be encapsulated into chitosan nanoparticles. Chitosan powder characteristic peaks were in agreement with previous studies (3, 13, 15, 31), and the interaction between EOs and CS was confirmed by previous studies (1, 3). The chitosan-carbomer complex is appropriate for entrapping and slow release of OEO. Beyki et al. (15) reported the sustained release of Mentha piperita EOs during four weeks, which agrees with our findings.

5.1. Conclusions

In this study, OEO-loaded CS nano-capsules were provided using the ionic gelation method. The size of the particles was below 200 nm with acceptable stability. The encapsulation efficiency was found more than 95%. As the OEO to chitosan weight ratio increased, LC% increased, while EE% decreased. The FTIR results confirmed the ionic complex between Cs and carbomer and demonstrated that OEO could be encapsulated into chitosan nanoparticles successfully. Moreover, the slow and sustainable in vitro release of OEO-CS nanoparticles during two weeks indicated that CS could be a potential candidate for the enhanced stability of plant EOs. The results confirmed the suitability of the CS-carbomer complex for OEO- CSNPs formation. Therefore, it will enhance the biomedical, pharmaceutical, and agricultural applications of these natural agents.

Acknowledgments

We would like to acknowledge the Department of Pharmacognosy, Ahvaz Jundishapur University of Medical Sciences, Iran, for the identification of the plant. We are grateful to Shahid Chamran University and Naft University for providing facilities to carry out the study.

Footnotes

Authors' Contribution: Mona Sharififard and Maryam Kouchak were responsible for the experiments. Ismaeil Alizadeh analyzed all data. Mona Sharififard and Elham Jahanifard designed the research and wrote the paper.

Conflict of Interests: The authors declare that they have no conflict of interest.

Ethical Approval: IR.AJUMS.REC.1395.752.

Funding/Support: This study was financially supported by the Infectious and Tropical Diseases Research Center, Health Research Institute, Ahvaz Jundishapur University of Medical Sciences with project No. OG-95137.

References

1. Abreu FO, Oliveira EF, Paula HC, de Paula RC. Chitosan/cashew gum nanogels for essential oil encapsulation. *Carbohydr Polym*. 2012;**89**(4):1277–82. doi: 10.1016/j.carbpol.2012.04.048. [PubMed: 24750942].
2. El Asbahani A, Miladi K, Badri W, Sala M, Ait Addi EH, Casabianca H, et al. Essential oils: from extraction to encapsulation. *Int J Pharm*. 2015;**483**(1-2):220–43. doi: 10.1016/j.ijpharm.2014.12.069. [PubMed: 25683145].
3. Hosseini SF, Zandi M, Rezaei M, Farahmandghavi F. Two-step method for encapsulation of oregano essential oil in chitosan nanoparticles: preparation, characterization and in vitro release study. *Carbohydr Polym*. 2013;**95**(1):50–6. doi: 10.1016/j.carbpol.2013.02.031. [PubMed: 23618238].
4. Ragaei M, Sabry AH. Nanotechnology for insect pest control. *Int J Sci Environ Technol*. 2014;**3**(2):528–45.
5. Woranuch S, Yoksan R. Eugenol-loaded chitosan nanoparticles: I. Thermal stability improvement of eugenol through encapsulation. *Carbohydr Polym*. 2013;**96**(2):578–85. doi: 10.1016/j.carbpol.2012.08.117. [PubMed: 23768603].
6. Haider J, Majeed H, Williams PA, Safdar W, Zhong F. Formation of chitosan nanoparticles to encapsulate krill oil (Euphausia superba) for application as a dietary supplement. *Food Hydrocolloids*. 2017;**63**:27–34. doi: 10.1016/j.foodhyd.2016.08.020.
7. Calvo P, Remun-Lpez C, Vila-Jato JL, Alonso MJ. Novel hydrophilic chitosan-polyethylene oxide nanoparticles as protein carriers. *J Appl Polym Sci*. 1997;**63**(1):125–32. doi: 10.1002/(sici)1097-4628(19970103)63:1<125::aid-app13>3.0.co;2-4.
8. Bhattacharyya A, Bhaumik A, Rani PU, Mandal S, Epidi TT. Nanoparticles-A recent approach to insect pest control. *Afr J Biotechnol*. 2010;**9**(24):3489–93.
9. Hsieh WC, Chang CP, Gao YL. Controlled release properties of Chitosan encapsulated volatile Citronella Oil microcapsules by thermal treatments. *Colloids Surf B Biointerfaces*. 2006;**53**(2):209–14. doi: 10.1016/j.colsurfb.2006.09.008. [PubMed: 17049821].
10. Flores FC, de Lima JA, Ribeiro RF, Alves SH, Rolim CM, Beck RC, et al. Antifungal activity of nanocapsule suspensions containing tea tree oil on the growth of Trichophyton rubrum. *Mycopathologia*. 2013;**175**(3-4):281–6. doi: 10.1007/s11046-013-9622-7. [PubMed: 23392821].
11. São Pedro A, Santo I, Silva C, Detoni C, Albuquerque E. The use of nanotechnology as an approach for essential oil-based formulations with antimicrobial activity. In: Méndez-Vilas A, editor. *Microbial Pathogens and Strategies for Combating Them*. **2**. Formatex Research Center Pulisher; 2013. p. 1364–74.
12. Negahban M, Moharramipour S, Zandi M, Hashemi SA. Efficiency of nanoencapsulated essential oil of Artemisia sieberi Besser on nutritional indices of Plutella xylostella. *Iran J Med Aromat Plants*. 2013;**29**(3).
13. Khan TA, Peh KK, Ch'ng HS. Reporting degree of deacetylation values of chitosan: the influence of analytical methods. *J Pharm Pharm Sci*. 2002;**5**(3):205–12. [PubMed: 12553887].
14. Hashemi SMB, Nikmaram N, Esteghlal S, Mousavi Khaneghah A, Niakousari M, Barba FJ, et al. Efficiency of Ohmic assisted hydrodistillation

for the extraction of essential oil from oregano (Origanum vulgare subsp. viride) spices. *Innovative Food Sci Emerg Technol*. 2017;**41**:172–8. doi: 10.1016/j.ifset.2017.03.003.
15. Beyki M, Zhaveh S, Khalili ST, Rahmani-Cherati T, Abollahi A, Bayat M, et al. Encapsulation of Mentha piperita essential oils in chitosan–cinnamic acid nanogel with enhanced antimicrobial activity against Aspergillus flavus. *Ind Crops Prod*. 2014;**54**:310–9. doi: 10.1016/j.indcrop.2014.01.033.
16. Mehdizadeh L, Najafgholi HM, Biouki RY, Moghaddam M. Chemical Composition and Antimicrobial Activity of Origanum vulgare subsp. viride Essential Oils Cultivated in Two Different Regions of Iran. *J Essent Oil Bear Plants*. 2018;**21**(4):1062–75. doi: 10.1080/0972060x.2018.1491329.
17. Andi SA, Nazeri V, Hadian J, Zamani Z. Chemical Composition of Essential Oil ofOriganum vulgaressp.viridefrom Iran. *J Essent Oil Bear Plants*. 2011;**14**(6):805–9. doi: 10.1080/0972060x.2011.10644008.
18. Afsharypour S, Sajjadi SE, Erfan-Manesh M. Volatile constituents of Origanum vulgare ssp. viride (syn. O. heracleoticum) from Iran. *Planta Med*. 1997;**63**(2):179–80. doi: 10.1055/s-2006-957640. [PubMed: 17252342].
19. Dewer Y, Mahmoud MM. Effectiveness and safety of some essential oils of aromatic plants on the growth and silk production of the silkworm Bombyx mori L. *L J Entomol Zool Stud*. 2014;**2**(2):81–6.
20. Adams RP. *Identification of essential oil components by gas chromatography/mass spectrometry*. **456**. Allured publishing corporation Carol Stream, IL; 2007.
21. Hashemi SMB, Mousavi Khaneghah A, Ghaderi Ghahfarrokhi M, Eş I. Basil-seed gum containing Origanum vulgare subsp. viride essential oil as edible coating for fresh cut apricots. *Postharvest Biol Technol*. 2017;**125**:26–34. doi: 10.1016/j.postharvbio.2016.11.003.
22. Ajun W, Yan S, Li G, Huili L. Preparation of aspirin and probucol in combination loaded chitosan nanoparticles and in vitro release study. *Carbohydr Polym*. 2009;**75**(4):566–74. doi: 10.1016/j.carbpol.2008.08.019.
23. Yoksan R, Jirawutthiwongchai J, Arpo K. Encapsulation of ascorbyl palmitate in chitosan nanoparticles by oil-in-water emulsion and ionic gelation processes. *Colloids Surf B Biointerfaces*. 2010;**76**(1):292–7. doi: 10.1016/j.colsurfb.2009.11.007. [PubMed: 20004558].
24. Kumaraswamy RV, Kumari S, Choudhary RC, Pal A, Raliya R, Biswas P, et al. Engineered chitosan based nanomaterials: Bioactivities, mechanisms and perspectives in plant protection and growth. *Int J Biol Macromol*. 2018;**113**:494–506. doi: 10.1016/j.ijbiomac.2018.02.130. [PubMed: 29481952].
25. Keawchaoon L, Yoksan R. Preparation, characterization and in vitro release study of carvacrol-loaded chitosan nanoparticles. *Colloids Surf B Biointerfaces*. 2011;**84**(1):163–71. doi: 10.1016/j.colsurfb.2010.12.031. [PubMed: 21296562].
26. Bhattacharjee S. DLS and zeta potential - What they are and what they are not? *J Control Release*. 2016;**235**:337–51. doi: 10.1016/j.jconrel.2016.06.017. [PubMed: 27297779].
27. Abdul Ghafoor Raja M, Katas H, Abd Hamid Z, Razali NA. Physicochemical Properties andIn VitroCytotoxicity Studies of Chitosan as a Potential Carrier for Dicer-Substrate siRNA. *J Nanomater*. 2013;**2013**:1–10. doi: 10.1155/2013/653892.
28. Chang SH, Lin HT, Wu GJ, Tsai GJ. pH Effects on solubility, zeta potential, and correlation between antibacterial activity and molecular weight of chitosan. *Carbohydr Polym*. 2015;**134**:74–81. doi: 10.1016/j.carbpol.2015.07.072. [PubMed: 26428102].
29. Jamil B, Abbasi R, Abbasi S, Imran M, Khan SU, Ihsan A, et al. Encapsulation of Cardamom Essential Oil in Chitosan Nanocomposites: In-vitro Efficacy on Antibiotic-Resistant Bacterial Pathogens and Cytotoxicity Studies. *Front Microbiol*. 2016;**7**:1580. doi: 10.3389/fmicb.2016.01580. [PubMed: 27757108]. [PubMed Central: PMC5048087].
30. Choudhary RC, Kumari S, Kumaraswamy RV, Pal A, Raliya R, Biswas P, et al. Characterization Methods for Chitosan-Based Nanomaterials. *Plant Nanobionics*. 2019. p. 103–16. doi: 10.1007/978-3-030-12496-0_5.
31. Vitali L, Justi KC, Laranjeira MC, Fávere VT. Impregnation of chelating agent 3,3-bis-N,N bis-(carboxymethyl)aminomethyl-o-cresolsulfonephthalein in biopolymer chitosan: adsorption equilibrium of Cu(II) in aqueous medium. *Polímeros*. 2006;**16**(2):116–22. doi: 10.1590/s0104-14282006000200011.